Quaternary Research (2021), **104**, 43–53
doi:10.1017/qua.2021.18

Research Article

Oxygen isotopes in terrestrial gastropod shells track Quaternary climate change in the American Southwest

Jason A. Rech[a]*, Jeffrey S. Pigati[b], Kathleen B. Springer[b], Stephanie Bosch[a], Jeffrey C. Nekola[c] and Yurena Yanes[d]

[a]Department of Geology and Environmental Earth Science, Miami University, Oxford OH 45056; [b]U.S. Geological Survey, Denver Federal Center, Box 25046, MS 980, Denver CO 80225; [c]Department of Ecology, Masaryk University, Brno, Czech Republic and [d]Department of Geology, University of Cincinnati, Cincinnati OH 45221

Abstract

Recent studies have shown the oxygen isotopic composition ($\delta^{18}O$) of modern terrestrial gastropod shells is determined largely by the $\delta^{18}O$ of precipitation. This implies that fossil shells could be used to reconstruct the $\delta^{18}O$ of paleo-precipitation as long as the isotopic system, including the hydrologic pathways of the local watershed and the gastropod systematics, is well understood. In this study, we measured the $\delta^{18}O$ values of 456 individual gastropod shells collected from paleowetland deposits in the San Pedro Valley, Arizona that range in age from ca. 29.1 to 9.8 ka. Isotopic differences of up to 2‰ were identified among the four taxa analyzed (Succineidae, *Pupilla hebes*, *Gastrocopta tappaniana*, and *Vallonia gracilicosta*), with Succineidae shells yielding the highest values and *V. gracilicosta* shells exhibiting the lowest values. We used these data to construct a composite isotopic record that incorporates these taxonomic offsets, and found shell $\delta^{18}O$ values increased by ~4‰ between the last glacial maximum and early Holocene, which is similar to the magnitude, direction, and rate of isotopic change recorded by speleothems in the region. These results suggest the terrestrial gastropods analyzed here may be used as a proxy for past climate in a manner that is complementary to speleothems, but potentially with much greater spatial coverage.

Keywords: Terrestrial gastropods, Oxygen isotopes, Paleoclimate, Paleowetland deposits

(Received 8 November 2020; accepted 26 February 2021)

INTRODUCTION

Earth has experienced episodes of abrupt climate change in the recent geologic past that are similar in direction and scale to those predicted for the future (IPCC, 2014). To better anticipate future climate variability and prepare for the potential impacts on society, the development of paleoclimatic proxies is needed to quantify the magnitude, spatial variability, and timing of past climatic fluctuations. A number of well-calibrated and robust geochemical proxies exist for marine settings (e.g., oxygen isotopes of foraminifera, Mg/Ca ratios of calcitic organisms, and organic biomarkers such as alkenones and glycerol dialkyl glycerol tetraether [GDGT] lipids), which have been key for reconstructing past changes in the oceans. Many of these proxies also have been applied to lacustrine systems in continental settings, but few quantitative proxies for past climate change are available for use in arid environments where perennial lakes are typically absent.

Over the past several decades, oxygen isotope ($\delta^{18}O$) records from speleothems have become an important terrestrial paleoclimatic proxy because of their ability to document climatic changes at exceptionally high temporal resolutions (Wang et al., 2001; Dykoski et al., 2005; Fleitmann et al., 2007). Speleothems have proven especially useful in arid environments, including those in the southwestern U.S., where they have been used to reconstruct the $\delta^{18}O$ of paleo-precipitation (Polyak et al., 2004, 2012; Asmerom et al., 2007, 2010, 2017; Wagner et al., 2010; Lachniet et al., 2014). Further, speleothem records have demonstrated that brief periods of aridity in the southwestern U.S. during the last glacial period coincided temporally with warm conditions in the North Atlantic, highlighting their role in understanding how abrupt changes in climate are propagated globally through atmospheric teleconnection processes (e.g., Wagner et al., 2010).

Despite their utility, speleothems are limited in spatial extent because only ~15% of the Earth's ice-free continental surface is characterized by carbonate rocks, and many of these cannot produce caves (Goldscheider et al., 2020). Moreover, most cave systems do not meet the requirements for oxygen isotopic equilibrium necessary to produce robust records of past climate (Quade, 2003). When the requirements are met, speleothems generally record the $\delta^{18}O$ of local paleo-precipitation, and are typically used to reconstruct past climates for the surrounding region, often without a quantitative understanding of how far the data can or should be extrapolated.

A potential source of paleoclimatic data that is complementary to speleothems is the $\delta^{18}O$ values of fossil terrestrial gastropod shells (Yapp, 1979; Lecolle, 1985; Goodfriend and Ellis, 2002; Balakrishnan and Yapp, 2004; Balakrishnan et al., 2005a, b; Yanes et al., 2009, 2011, 2013; Paul and Mauldin, 2013). Gastropods are one of the most abundant fossil groups in the terrestrial geologic record and their shells are preserved in a wide variety of depositional settings, including loess, eolian sand,

*Corresponding author: Jason A. Rech, Email: rechja@miamioh.edu

Cite this article: Rech JA, Pigati JS, Springer KB, Bosch S, Nekola JC, Yanes Y (2021). Oxygen isotopes in terrestrial gastropod shells track Quaternary climate change in the American Southwest. *Quaternary Research* **104**, 43–53. https://doi.org/10.1017/qua.2021.18

alluvial and fluvial sequences, and geologic deposits associated with desert wetland ecosystems. Their abundance, preservation, and broad spatial and temporal coverage make fossil gastropod shells a potentially important archive of past environmental and climatic conditions in the terrestrial realm, provided the isotopic system is well constrained (Goodfriend and Ellis, 2002; Yanes et al., 2009; Nash et al., 2018; Grimley et al., 2020).

Terrestrial gastropod shells are composed primarily of aragonite ($CaCO_3$), and their $\delta^{18}O$ values depend on local climatic and environmental parameters at the time of shell formation (Balakrishnan and Yapp, 2004). Shell $\delta^{18}O$ values can be affected by several atmospheric variables that vary between ecological habitats and even microhabitats, including $\delta^{18}O$ of precipitation, temperature, $\delta^{18}O$ of water vapor, and relative humidity. These values also are affected by the proportion of water derived from different hydrologic pathways (e.g., direct precipitation, dew, surface water, groundwater discharge) that are utilized by gastropods. Despite these potential complexities, a recent study of modern small (<10 mm) terrestrial gastropods in North America has shown that the $\delta^{18}O$ value of local precipitation is the dominant driver of shell $\delta^{18}O$ values (Yanes et al., 2019). Therefore, much like speleothems, fossil gastropod shells have the potential to track changes in the $\delta^{18}O$ of paleo-precipitation through time, but over much broader spatial scales.

In this study, we measured the $\delta^{18}O$ values of 456 fossil gastropod shells collected from late Pleistocene and early Holocene paleowetland deposits in southeastern Arizona. These data were analyzed and compared with independent $\delta^{18}O$ records derived from speleothems in the American Southwest to determine if gastropod shell $\delta^{18}O$ values track the same environmental trends over geologic timescales. If so, this would allow researchers to obtain paleoclimate information that is complementary to speleothems, thereby improving our understanding of past climate conditions in arid environments.

STUDY AREA

The San Pedro Valley of southeastern Arizona is located in the southernmost portion of the Basin and Range Province, at the border between the Sonoran and Chihuahuan deserts (Fig. 1a). Late Pleistocene and early Holocene paleowetland deposits are exposed discontinuously over ~150 km of the roughly north-south valley and represent periods of high water table conditions resulting from increased effective precipitation and groundwater recharge (Pigati et al., 2004, 2009). The deposits are especially prevalent in the southwest part of the valley, where groundwater is fed by precipitation falling in the Huachuca Mountains to the west, which include peaks of Paleozoic sedimentary rocks that exceed 3000 m in elevation (Reynolds, 1988).

In the late 1800s, rapid erosion and valley head cutting caused a precipitous drop in water table levels in the San Pedro Valley and surrounding areas (Cooke and Reeves, 1976; Waters and Haynes, 2001). At this time, arroyos formed as streams incised into alluvial fan sediments along the eastern flanks of the Huachuca Mountains. This exposed an unusually complete sequence of late Quaternary paleowetland deposits at a number of sites on the west side of the valley (Haynes, 1968, 1987, 2007). The sediments include marls and organic-rich silts informally referred to as "black mats," which represent spring ecosystems (e.g., marshes and wet meadows) that prevailed in the valley during wetter times (Pigati et al., 2004, 2009). Fossil gastropods are most abundant in the carbonate-rich marls of these depositional sequences, which represent periods of greatest groundwater discharge. Gastropod shells are less commonly preserved in black mats, which is likely the result of acidic conditions in these organic-rich deposits rather than lack of original prevalence.

METHODS

Collection and cleaning of fossil shells

Fossil gastropod shells analyzed in this study were collected from marls at three sites within the San Pedro Valley, including Murray Springs, Lehner Ranch, and Lindsey Ranch, and from a black mat at Lindsey Ranch (Fig. 1b). At Murray Springs and Lehner Ranch, bulk samples of marl containing fossil gastropod shells were collected in 10-cm intervals at the same locations where Succineidae shells were collected previously for dating. Samples also were collected in 10-cm intervals from a previously undated marl and black mat at Lindsey Ranch. In all cases, shells were extracted from the host sediment by placing the samples in a plastic bin with water and putting them through a series of 5–10 freeze-thaw cycles on a daily basis. Once the marl was disaggregated and softened, the samples were wet-sieved through a 600 µm mesh screen, which allowed us to pick the shells and sort them taxonomically based on morphological features. The shells were then identified to the most precise taxonomic level possible, to species in most cases, with the exception of shells attributed to the Succineidae family. Succineidae shells exhibit few diagnostic characteristics and taxonomic identification is based on soft-body reproductive organ morphology, which is not preserved in the fossil record. Identification of these shells was therefore limited to the family level.

Methods for additional cleaning were determined based on the thickness and durability of the shell material. Succineidae shells were the largest and most robust, so were cleaned using an ultrasonic bath for 10–20 seconds, followed by multiple rinses with deionized water until the shells were free of detrital material. Shells of the other taxa were smaller and more fragile, so the ultrasonic bath was not used to avoid damaging them. This was a key concern because these other taxa were also limited in abundance. The smaller shells were soaked in a 1% Alconox solution for 30 minutes to remove sediment adhering to shells, and then rinsed with deionized water. All shells were dried at room temperature for at least 24 hours and then examined with a microscope for cleanliness. This process was repeated until the shells were visually free of detritus.

Radiocarbon dating

Age control for the marls at Murray Springs and Lehner Ranch was determined previously using accelerator mass spectrometry (AMS) ^{14}C dating of Succineidae shells (Pigati et al., 2004, 2009). Radiocarbon dating of Succineidae shells and organic matter was also used to determine the ages of the marl and black mat at Lindsey Ranch using the following procedures. Clean shell carbonate was partially leached with HCl to remove any secondary carbonate and then converted to CO_2 using American Chemical Society (ACS) reagent grade 85% H_3PO_4 under vacuum at 50°C until the reaction was visibly complete (ca. 1 hour). Organic matter was treated using the standard acid-base-acid (ABA) procedure before being washed with ASTM Type 1, 18.2 MΩ water, dried, and combusted online at 625°C in the presence of excess

https://doi.org/10.1017/qua.2021.18 Published online by Cambridge University Press

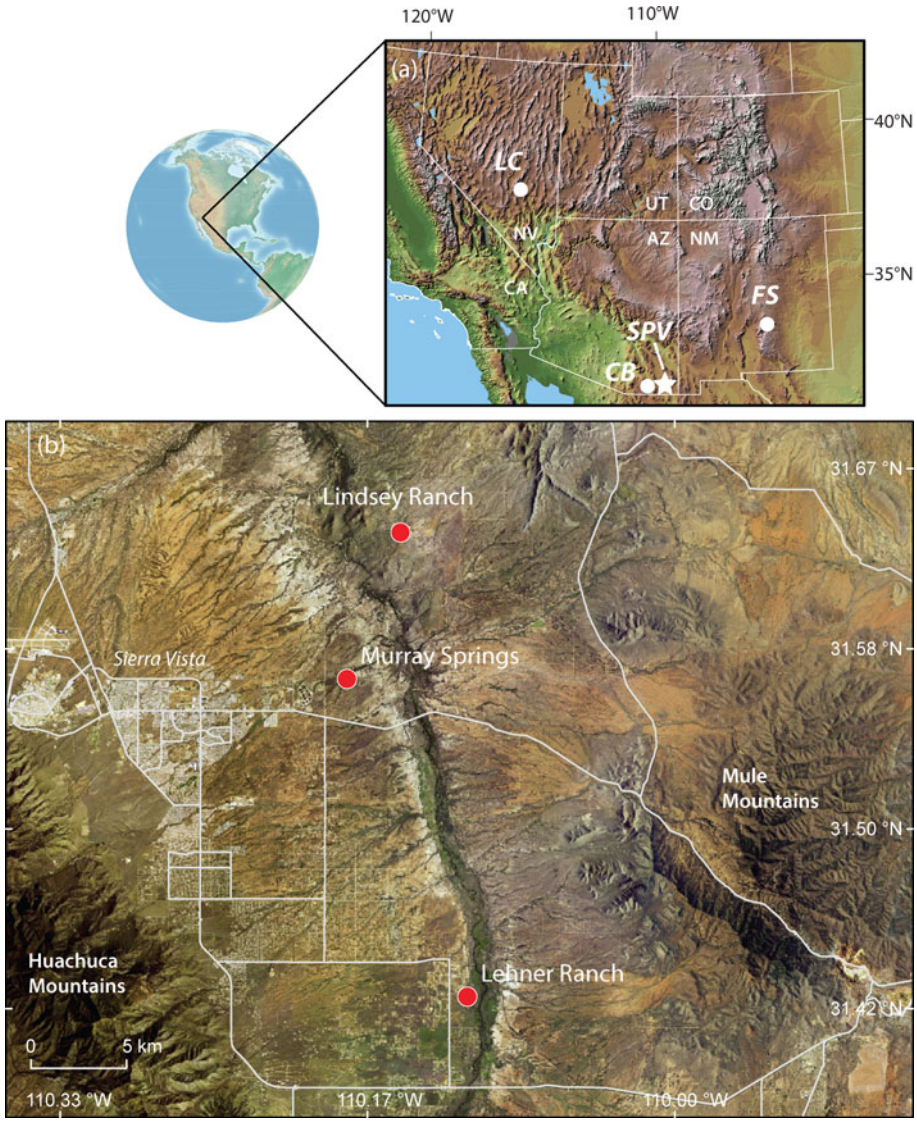

Figure 1. (a) Location of the San Pedro Valley (SPV; denoted by white star) and key speleothems in the region (white circles); LC = Leviathan Cave, NV (Lachniet et al., 2014); CB = Cave of the Bells, AZ (Wagner et al., 2010); FS = Fort Stanton Cave, NM (Asmerom et al., 2010). Western states shown include California (CA), Nevada (NV), Arizona (AZ), New Mexico (NM), Colorado (CO), and Utah (UT). (b) Landsat image from 2017 of the southern part of the valley showing the locations of sampling sites (red circles). Landsat image is courtesy of the U.S. Geological Survey's Earth Resources Observation and Science Center. (For interpretation of the references to color in this figure legend, the reader is referred to the web version of this article.)

high-purity oxygen. For all samples, water and other contaminant gases were removed by cryogenic separation, and the resulting purified CO_2 gas was measured manometrically and converted to graphite via hydrogen reduction using an iron catalyst (Vogel et al., 1984). Carbon isotope ratios of the graphite targets were measured by AMS, and the resulting ^{14}C ages, as well as those reported by Pigati et al. (2004, 2009), were calibrated using the IntCal20 dataset and CALIB 8.2 (Reimer et al., 2020; Stuiver et al., 2020). Ages are presented in thousands of calibrated years (ka) before present (BP; 0 yr BP = 1950 AD), and uncertainties are given at the 95% (2σ) confidence level.

For the Murray Springs chronology, a few of the ages at depths between 40 and 110 cm were either statistically indistinguishable from those above or below or did not maintain stratigraphic order (Table 1; Fig. 2a). Therefore, we used Bacon v. 2.2 modeling software (Blaauw and Christen, 2011) to construct an age-depth model for this interval (Supplementary Figure 1).

Oxygen isotope geochemistry

Oxygen isotopes of the fossil gastropod shells were measured at the Department of Earth and Planetary Sciences Stable Isotope Laboratory at the University of New Mexico using the method described by Spotl and Vennemann (2003). Briefly, each shell was powdered to homogenize the sample and ~200 µg of shell aragonite was loaded into 12-ml borosilicate Exetainer® vials. The vials were flushed with helium and then allowed to react for 24 hours with phosphoric acid (H_3PO_4) at 50°C. The evolved CO_2 was measured by continuous flow isotope ratio mass spectrometry using a Thermo Scientific™ GasBench device coupled to a Finnigan Mat Delta V isotope ratio mass spectrometer. The results are reported using the standard delta notation against the VPDB standard (Coplen et al., 2006). Reproducibility was better than 0.15‰ for both $\delta^{13}C$ and $\delta^{18}O$ based on repeated measurements of the Carrara Marble standard (IAEA-CO-1).

https://doi.org/10.1017/qua.2021.18 Published online by Cambridge University Press

Table 1. Summary of AMS sample information, ^{14}C ages, and calibrated ages. Uncertainties for the calibrated ages are given at the 2σ (95%) confidence level. All other uncertainties are given at 1σ (68%).

Sample #	AMS #	Context	Material dated	Treatment[1]	^{14}C age (^{14}C ka BP)	Cal age (ka BP)[2]	P[3]	Source[4]
Lindsey Ranch								
LiR 0-10	CAMS-174486	sediment	Succineidae	HCl	8.78 ± 0.03	9.78 ± 0.13	0.96	1
LiR 20-30	CAMS-174485	sediment	Succineidae	HCl	9.23 ± 0.03	10.39 ± 0.12	0.99	1
LiR 40-50	Aeon-2171	black mat	organics	ABA	9.68 ± 0.05	10.88 ± 0.01	0.35	1
						11.14 ± 0.07	0.62	1
Lehner Ranch								
LeR 0-10	AA-61001	sediment	Succineidae	HCl	14.30 ± 0.05	17.32 ± 0.21	0.95	2
LeR 40-50	AA-60999	sediment	Succineidae	HCl	16.31 ± 0.07	19.70 ± 0.18	1.00	2
Murray Springs								
MS 0-10	AA-39316	sediment	Succineidae	HCl	17.86 ± 0.08	21.69 ± 0.28	1.00	3
MS 0-10 (r)	AA-39317	sediment	Succineidae	HCl	18.16 ± 0.08	22.12 ± 0.19	1.00	3
MS 10-20	AA-39326	sediment	Succineidae	HCl	19.38 ± 0.11	23.26 ± 0.21	0.65	3
						23.62 ± 0.13	0.35	3
MS 20-30	AA-39327	sediment	Succineidae	HCl	21.03 ± 0.10	25.40 ± 0.26	1.00	3
MS 30-40	AA-39319	sediment	Succineidae	HCl	21.60 ± 0.12	25.87 ± 0.19	1.00	3
MS 40-50	AA-39328	sediment	Succineidae	HCl	23.57 ± 0.12	27.66 ± 0.24	1.00	3
MS 50-60	AA-39329	sediment	Succineidae	HCl	23.69 ± 0.13	27.91 ± 0.30	1.00	3
MS 60-70	AA-39330	sediment	Succineidae	HCl	24.42 ± 0.14	28.66 ± 0.41	1.00	3
MS 70-80	AA-39331	sediment	Succineidae	HCl	24.98 ± 0.14	29.28 ± 0.43	1.00	3
MS 80-90	AA-39318	sediment	Succineidae	HCl	24.47 ± 0.12	28.73 ± 0.33	1.00	3
MS 90-100	AA-39333	sediment	Succineidae	HCl	24.62 ± 0.14	28.90 ± 0.26	1.00	3
MS 100-110	AA-39321	sediment	Succineidae	HCl	24.86 ± 0.17	29.13 ± 0.42	1.00	3
MS 100-110 (r)	AA-39320	sediment	Succineidae	HCl	24.31 ± 0.18	28.43 ± 0.50	1.00	3

[1]ABA = acid-base-acid; HCl = acid leach.
[2]Calibrated ages were calculated using CALIB v.8.2html, IntCal20.14C dataset; limit 55.0 calendar ka B.P. Calibrated ages are reported as the midpoint of the calibrated range. Uncertainties are reported as the difference between the midpoint and either the upper or lower limit of the calibrated age range, whichever is greater. Ages are reported when the probability of a calibrated age range exceeds 0.05.
[3]P = probability of the calibrated age falling within the reported range as calculated by CALIB.
[4]1 = this study; 2 = Pigati et al., 2009; 3 = Pigati et al., 2004.

RESULTS

Stratigraphy and chronology

At Murray Springs, the Coro Marl member of the Murray Springs formation of Haynes (1968, 2007), which has been alternately referred to as Unit E and the upper member of the Boquillas formation by Haynes (1968), is ~110 cm thick and consists of massive, hard, white to light-gray, calcareous silty clay (marl) that contains abundant fossil shells of terrestrial and aquatic gastropods (Fig. 2a). This unit dates to ca. 29.1–21.7 ka based on ^{14}C ages of Succineidae shells originally reported by Pigati et al. (2004) and recalibrated here using the IntCal20 calibration curve (Reimer et al., 2020; Stuiver et al., 2020) (Table 1). Our new examination of the sequence at Murray Springs identified that the Coro marl does not represent a continuous depositional sequence as previously reported, but rather contains a stratigraphic break in the marl marked by a contact with a light-green silty clay with prismatic structure at a depth of ~40 cm below the top of the unit. This break is bounded by calibrated ^{14}C ages of 27.66 ± 0.24 ka and 25.87 ± 0.19 ka (Fig. 2a; Table 1).

At Lehner Ranch, fossil shells were collected from a hard, light-gray marl that is ~50 cm thick (Fig. 2b). This unit was also called Unit E by Haynes (1968) and was incorrectly attributed to the Coro marl by Pigati et al. (2009), as it dates to between ca. 19.7 and 17.3 ka based on ^{14}C ages of Succineidae shells originally reported in Pigati et al. (2009) and recalibrated here (Table 1). Although the marl at Lehner Ranch was deposited in a similar environment (marshes and wet meadows) as the Coro marl at Murray Springs, it is significantly younger and therefore is not an equivalent unit.

Fossil gastropod shells were collected at Lindsey Ranch from a thin black mat and an overlying massive, light-gray marl that is ~50 cm thick (Fig. 2c), both of which are indicative of a marsh or wet meadow setting. Calibrated ^{14}C ages from organic matter within the black mat at Lindsey Ranch yielded multiple calibrated age ranges, with 11.14 ± 0.07 ka having the highest probability, and Succineidae shells from the overlying marl produced calibrated ages of 10.39 ± 0.12 ka at the bottom and 9.78 ± 0.13 ka at the top (Fig. 2; Table 1). Although the marl at Lindsey Ranch was also called Unit E by Haynes (1968), these new ages show that it is actually much younger than paleowetland

https://doi.org/10.1017/qua.2021.18 Published online by Cambridge University Press

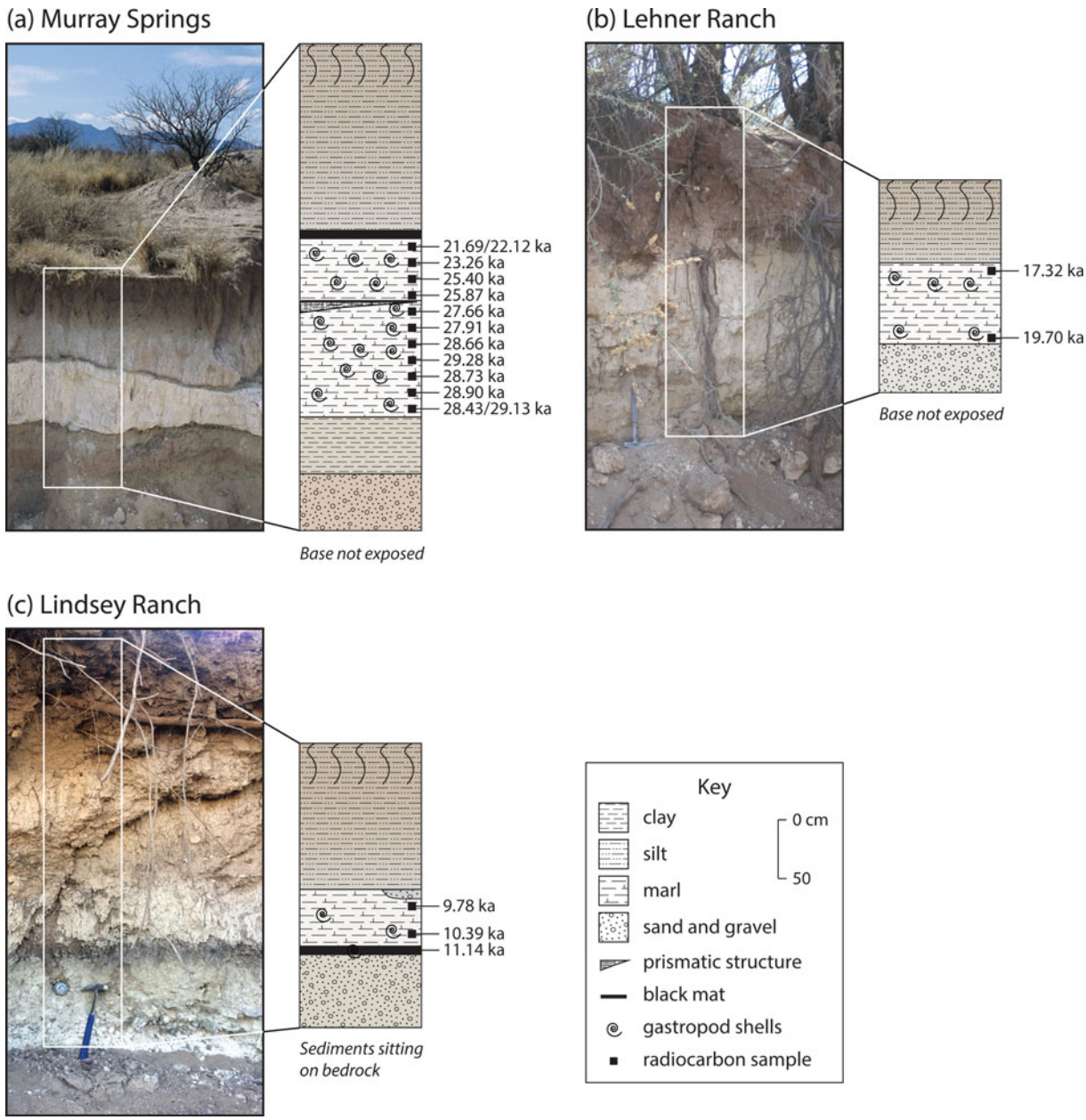

Figure 2. (color online) Stratigraphy, calibrated ages (in ka), and photographs of sediments at (a) Murray Springs, (b) Lehner Ranch, and (c) Lindsey Ranch. Photographs courtesy of Jeff Pigati.

deposits referred to as Unit E elsewhere in the San Pedro Valley, and is also younger than the marl at Lehner Ranch.

Finally, we note that the 10-cm sampling units utilized in this study represent various time intervals because the deposits at the three sites have different sedimentation rates. At Murray Springs, for example, 10 cm represents 600–1200 years (depending on the sample depth), whereas the same sampling interval represents ca. 200 and 400 years at Lehner Ranch and Lindsey Ranch, respectively.

Isotopic results

Terrestrial gastropod shells recovered from the full glacial deposits at Murray Springs and late glacial deposits at Lehner Ranch were consistent with assemblages documented by Mead (2007) and include *Euconulus fulvus*, *Gastrocopta cristata*, *Gastrocopta tappaniana*, *Pupilla hebes*, *Pupilla sonorana*, *Pupoides hordaceus*, Succineidae, *Vallonia gracilicosta*, and *Vertigo berryi*. Individual shells of the aquatic snails *Fossaria* sp. and *Gyraulus* sp. also were recovered, as was the aquatic bivalve *Pisidium* sp. At Lindsey Ranch, gastropod shells were more limited and included Succineidae and *G. tappaniana*, as well as a few *Fossaria* sp. and rare *Pupilla* sp.

Shells of Succineidae (n = 156), *P. hebes* (n = 75), *V. gracilicosta* (n = 83), and *G. tappaniana* (n = 142) were chosen for isotopic analysis because they were the most abundant (Fig. 3) and have been validated as reliable paleoenvironmental proxies in North America (Yanes et al., 2017). All four taxa were analyzed from the marls at Murray Springs and Lehner Ranch, whereas only

https://doi.org/10.1017/qua.2021.18 Published online by Cambridge University Press

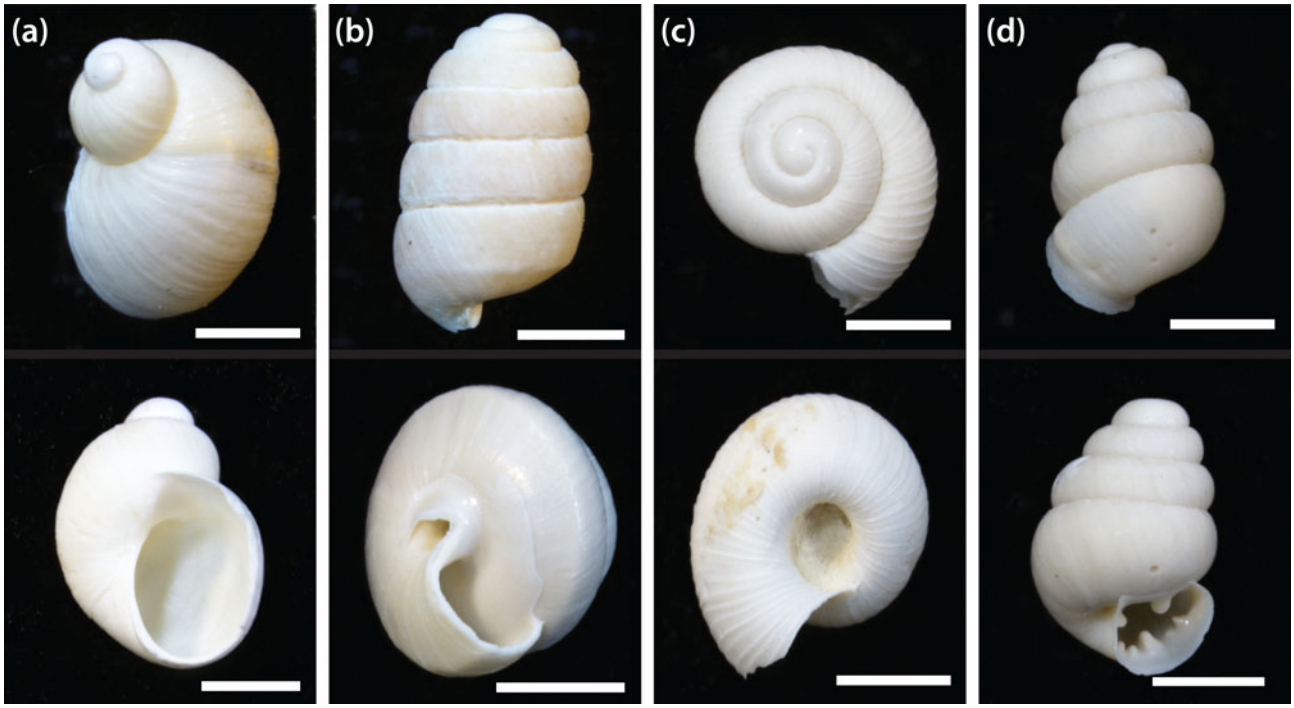

Figure 3. (color online) Photographs of select fossil gastropod taxa collected from Murray Springs. Scale bars are all 1 mm in length. (a) Succineidae; (b) *Pupilla hebes*; (c) *Vallonia gracilicosta*; and (d) *Gastrocopta tappaniana*. Photographs courtesy of Stephanie Bosch.

Succineidae and *G. tappaniana* were analyzed from Lindsey Ranch. For each sampling interval, we measured 10 individual shells of the same taxon, unless there were fewer than 10 shells, in which case we analyzed all available shells. In total, we measured 456 fossil shells from the three sites, including 359 shells from Murray Springs, 37 shells from Lehner Ranch, and 60 shells from Lindsey Ranch (Supplementary Table 1).

The $\delta^{18}O$ values generally increase over time, as shells from the full glacial age Coro marl at Murray Springs yielded the lowest isotopic values, shells from the late glacial marl at Lehner Ranch yielded intermediate values, and shells from the early Holocene black mat and marl at Lindsey Ranch yielded the highest values (Table 2; Fig. 4a–d). We also observed a range of ~2.5–4.0‰ in the $\delta^{18}O$ values of fossil shells between individual taxa within each sampling interval (Supplementary Table 1). However, $\delta^{18}O$ values for shells of the same taxa within a given interval were relatively consistent; standard deviations of data with $n > 5$ averaged ~1‰ and were similar between taxa: 1.26‰ for Succineidae ($n = 16$), 0.87‰ for *P. hebes* ($n = 6$), 0.98‰ for *V. gracilicosta* ($n = 8$), and 0.79‰ for *G. tappaniana* ($n = 14$).

Much of the observed isotopic variability within a given sampling interval is the result of differences between the four taxa (Table 2; Fig. 4e). The specific cause(s) of this variability is unknown, but may reflect small differences in micro-habitats, snail ecology, and possibly vital effects. Regardless, the magnitude of these inter-taxa isotopic differences is similar to those documented by Yanes et al. (2017) who found systematic offsets of 2–3‰ in $\delta^{18}O$ values between modern Succineidae, *V. gracilicosta*, and *G. tappaniana* in Minnesota, USA. In our study, inter-taxa differences of the fossil shells are consistent across location and time, with Succineidae always yielding the highest $\delta^{18}O$ values, *P. hebes* typically yielding the next highest values, and either *G. tappaniana* or *V. gracilicosta* yielding the lowest.

To quantify these differences, we determined isotopic offsets of Succineidae, *P. hebes*, and *V. gracilicosta* relative to *G. tappaniana*, which was the most common taxon identifiable to the species level. Offsets for the individual taxa were -1.92 ± 0.55‰ for Succineidae, -1.21 ± 0.51‰ for *P. hebes*, and +0.01 ± 0.22‰ for *V. gracilicosta* (Supplementary Table 2). We then calculated normalized $\delta^{18}O$ values by subtracting the isotopic offsets for Succineidae, *P. hebes*, and *V. gracilicosta*, and determined the average $\delta^{18}O$ value for all shells in a given 10-cm sampling interval (Supplementary Table 1; Table 2; Fig. 4f).

DISCUSSION

The composite isotopic record reveals that fossil gastropod $\delta^{18}O$ values increased by ~2‰ between the last glacial maximum and the late glacial period, and another ~2‰ between the late glacial period and the early Holocene (Table 2; Fig. 4f). Previous studies have shown that shell $\delta^{18}O$ values of the taxa analyzed here are determined largely by the $\delta^{18}O$ of precipitation (Yanes et al., 2019), but they could also be affected to a lesser degree by other atmospheric variables, including temperature, the $\delta^{18}O$ of water vapor, and relative humidity (Balakrishnan and Yapp, 2004). Increases in temperature between the late Pleistocene and early Holocene would have reduced isotopic fractionation during shell formation and caused shell $\delta^{18}O$ values to decrease over time, which is the opposite of what we observe in our record. Therefore, the influence of temperature on fractionation during shell formation is not a driving factor. Similarly, the $\delta^{18}O$ of water vapor and relative humidity should be relatively constant in perennial wetland ecosystems because of the continuous availability of water, so it is unlikely that these parameters varied enough to significantly affect the isotopic composition of the

https://doi.org/10.1017/qua.2021.18 Published online by Cambridge University Press

Table 2. Summary of measured and normalized $\delta^{18}O$ values[1].

		Average measured values for each taxon													Average normalized values for each taxon[2]				Average normalized values for all taxa	
		Succineidae			*P. hebes*			*V. gracilicosta*			*G.tappaniana*			Total	Succineidae	*P. hebes*	*V. gracilicosta*	*G.tappaniana*		
Sample ID	Cal age (ka)[3]	$\delta^{18}O$	± (1σ)	n	$\delta^{18}O$	± (1σ)	n	$\delta^{18}O$	± (1σ)	n	$\delta^{18}O$	± (1σ)	n	n	$\delta^{18}O$	$\delta^{18}O$	$\delta^{18}O$	$\delta^{18}O$	$\delta^{18}O$	± (1σ)[4]
Lindsey Ranch																				
LiR 0-10	9.78 ± 0.13	0.16	1.85	10	--	--	--	--	--	--	−1.71	0.91	10	20	−1.76	--	--	−1.71	−1.73	1.42
LiR 20-30	10.39 ± 0.12	−0.47	1.87	10	--	--	--	--	--	--	−1.76	0.68	10	20	−2.39	--	--	−1.76	−2.07	1.41
LiR 40-50	11.05 ± 0.11	−0.13	0.67	10	--	--	--	--	--	--	−1.44	1.00	10	20	−2.05	--	--	−1.44	−1.74	0.88
Lehner Ranch																				
LeR 0-10	17.32 ± 0.21	−2.49	1.80	10	−5.50	--	1	−5.01	1.44	5	−5.25	1.52	4	20	−4.41	--	--	--	−4.84	1.63
LeR 40-50	19.70 ± 0.18	−2.05	2.12	8	−4.82	--	1	−5.31	1.37	6	−3.95	2.38	2	17	−3.97	--	−5.30	--	−4.56	1.86
Murray Springs																				
MS 0-10	21.91 ± 0.34[5]	−4.68	0.67	10	−6.67	0.53	2	−6.98	0.96	5	−6.47	0.55	9	26	−6.60	--	--	−6.47	−6.72	0.75
MS 10-20	23.38 ± 0.25	−4.20	1.14	10	−4.86	0.80	10	−7.06	0.97	10	−7.13	0.89	10	40	−6.12	−6.07	−7.05	−7.13	−6.59	1.05
MS 20-30	25.40 ± 0.26	−5.32	0.64	10	−5.85	1.17	10	−7.08	1.14	10	−6.86	0.75	10	40	−7.24	−7.06	−7.07	−6.86	−7.06	0.93
MS 30-40	25.87 ± 0.19	−4.53	0.91	10	−5.78	0.73	6	−6.68	1.11	9	−6.98	0.60	10	35	−6.45	−6.99	−6.67	−6.98	−6.75	0.86
MS 40-50	*27.84 ± 0.32*	−4.56	0.77	9	−5.35	0.81	9	−6.66	0.46	10	−6.54	0.67	7	35	−6.48	−6.56	−6.65	−6.54	−6.56	0.66
MS 50-60	*28.06 ± 0.30*	−5.01	1.66	10	−6.24	0.80	5	--	--	--	−6.73	0.61	10	25	−6.93	--	--	−6.73	−6.96	1.16
MS 60-70	*28.32 ± 0.33*	−3.73	1.28	10	--	--	--	−6.79	0.80	6	−6.60	0.88	10	26	−5.65	--	−6.78	−6.60	−6.28	1.12
MS 70-80	*28.54 ± 0.30*	−4.87	1.39	10	−5.34	0.79	10	−6.19	1.33	9	−6.01	0.54	10	39	−6.79	−6.55	−6.18	−6.01	−6.39	1.07
MS 80-90	*28.71 ± 0.25*	−4.30	0.96	9	−5.63	1.19	10	−5.78	0.48	2	−6.54	0.78	10	31	−6.22	−6.84	--	−6.54	−6.50	0.98
MS 90-100	*28.88 ± 0.22*	−4.87	1.38	10	−5.53	0.63	6	−6.48	0.62	10	−6.75	0.96	10	36	−6.79	−6.74	−6.47	−6.75	−6.68	0.95
MS 100-110	*29.03 ± 0.23*	−4.50	1.11	10	−4.90	1.20	5	−5.05	--	1	−6.31	1.23	10	26	−6.42	--	--	−6.31	−6.27	1.14

[1]All $\delta^{18}O$ values are reported relative to the VPDB standard; uncertainties are reported as the standard deviation from the mean.
[2]Individual normalized values were calculated using the following offsets relative to *G. tappaniana* : Succineidae, -1.92 ± 0.55‰; *P. hebes*, -1.21 ± 0.51‰; *V. gracilicosta*, +0.01 ± 0.22‰.
[3]Ages in regular font are standard calibrated ages; those presented in italics are the product of Bacon age-depth modeling. See Supplementary Figure 1 for details.
[4]Uncertainties include all internal and external sources of error. See Supplementary Tables 1 and 2 for details.
[5]Average of two calibrated ages at this depth interval (see Table 1 for individual ages).

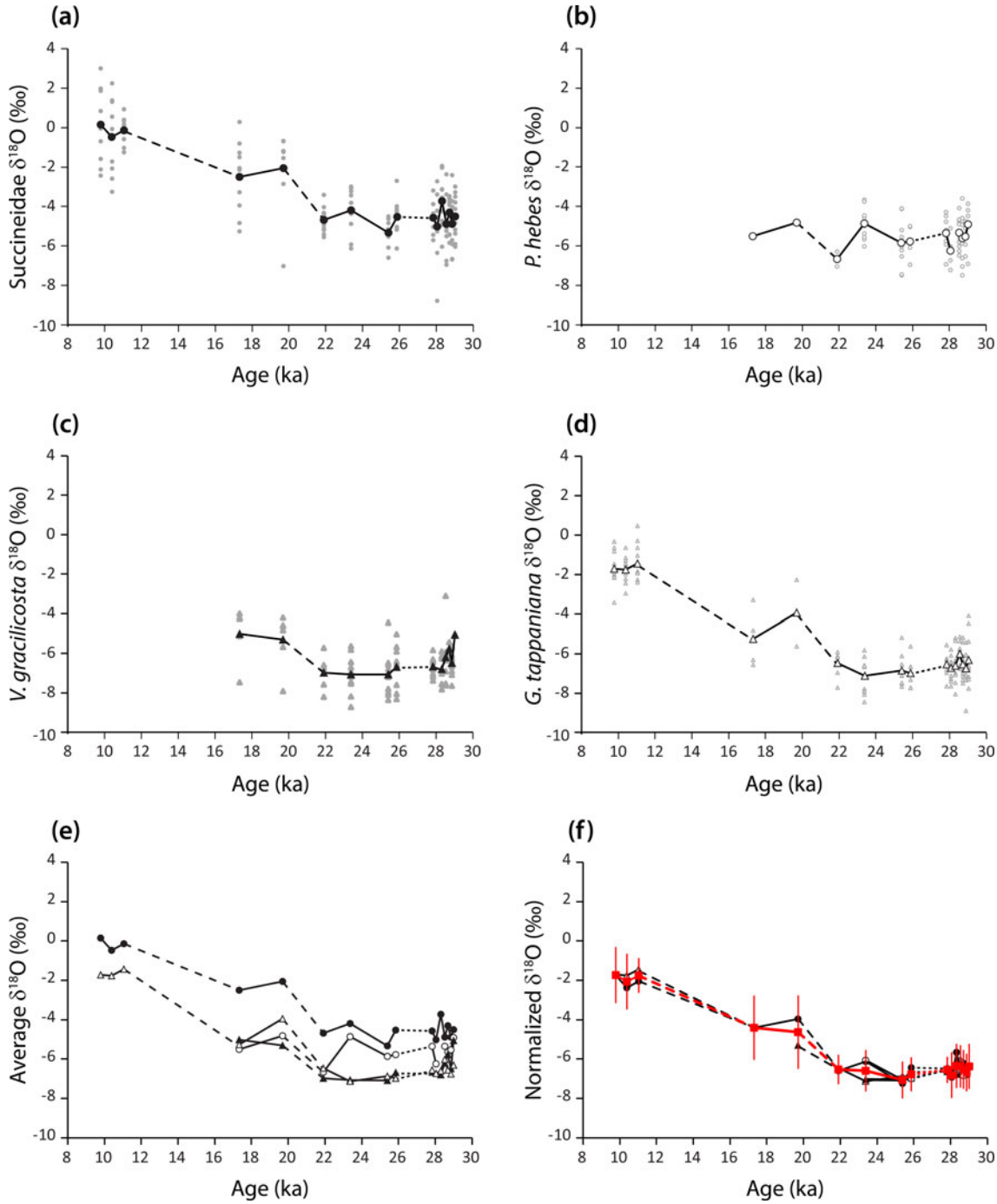

Figure 4. $\delta^{18}O$ values of fossil gastropod shells. Individual data points are shown in light gray; average values at each sampling interval are shown in black. Solid lines connect isotopic values from the same site; dashed lines connect data from different sites; dotted lines connect values across the depositional hiatus at Murray Springs. (a) Succineidae; (b) *Pupilla hebes*; (c) *Vallonia gracilicosta*; (d) *Gastrocopta tappaniana*; (e) average values for each taxon plotted together; (f) average $\delta^{18}O$ values normalized against *G. tappaniana* values for each taxon (shown in black) and average normalized $\delta^{18}O$ values for all taxa (shown in red). Uncertainties in the normalized $\delta^{18}O$ values are given at the 68% (1σ) confidence level. All plotted ages are given as calibrated ages (in ka). (For interpretation of the references to color in this figure legend, the reader is referred to the web version of this article.)

gastropod shells. Consequently, we interpret the changes observed in the composite isotopic record to reflect changes primarily in the $\delta^{18}O$ of precipitation.

The observed trends in the $\delta^{18}O$ values of the fossil gastropod shells suggest they have utility as a paleoclimate proxy record by tracking changes in the oxygen isotopic composition of paleoprecipitation over time in this region. Today, the climate of the San Pedro Valley is semi-arid, with average monthly high temperatures that range from ~33°C in the summer months (JJA) to ~17°C in the winter (DJF), and mean annual precipitation of ~36 cm/yr (https://www.usclimatedata.com/climate/sierra-vista/arizona/united-states/usaz0214; accessed 9/6/20). The effect of the North American monsoon on the seasonal distribution of precipitation is clear—nearly 60% of the annual precipitation

https://doi.org/10.1017/qua.2021.18 Published online by Cambridge University Press

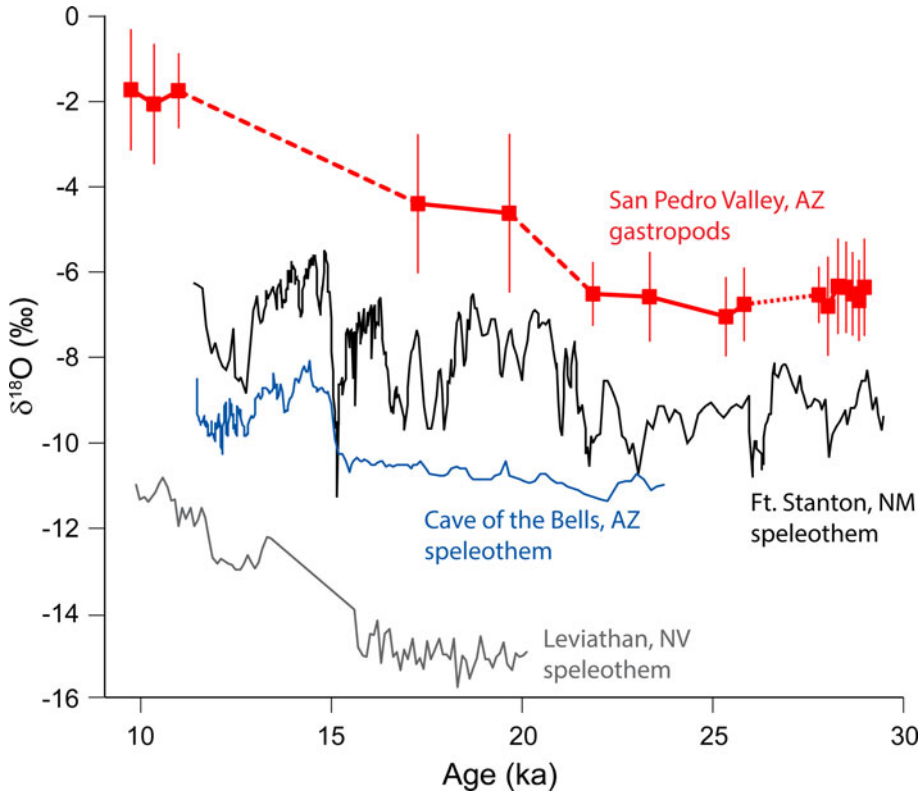

Figure 5. Average normalized shell $\delta^{18}O$ values for all gastropod taxa from the San Pedro Valley (red) compared to isotopic records of speleothems from Fort Stanton, NM (Asmerom et al., 2010), Cave of the Bells, AZ (Wagner et al., 2010), and Leviathan Cave, NV (Lachniet et al., 2014). As in Figure 4, solid lines connect gastropod shell $\delta^{18}O$ values from same site; dashed lines connect data from different sites; dotted lines connect values across the depositional hiatus at Murray Springs. All plotted ages are given as calibrated ages (in ka). (For interpretation of the references to color in this figure legend, the reader is referred to the web version of this article.)

falls between July and September with the remainder falling mostly between December and February. During the late Pleistocene and early Holocene, however, the strength of the North American monsoon was likely much less than today (Metcalfe et al., 2015), so annual precipitation in the valley was probably dominated by winter precipitation, as it was throughout much of the southwestern U.S. at that time (Lora and Ibarra, 2019).

The distribution of modern winter precipitation in the southwestern U.S. is characterized by a pronounced north-south dipole pattern in which conditions at latitudes north of ~40–42°N are generally wet whereas those to the south are relatively dry (Wise, 2010). The position of this dipole boundary is controlled by the interaction of westerly storm tracks and the atmosphere over the Pacific and Atlantic oceans, and has been hypothesized to be a fairly stable feature of western U.S. climate during the Quaternary (Hudson et al., 2019). This implies that during the late Pleistocene and early Holocene, paleoclimate proxies from sites located well south of ~40–42°N latitude should record similar paleoclimatic information, at least at broad temporal and spatial scales.

Three speleothem $\delta^{18}O$ records from south of this boundary in the American Southwest were chosen for comparison with the San Pedro Valley gastropod $\delta^{18}O$ data, including the nearby Cave of the Bells in southern Arizona (Wagner et al., 2010), Fort Stanton Cave, New Mexico (Asmerom et al., 2010), and Leviathan Cave, Nevada (Lachniet et al., 2014) (see Fig. 1a for locations). These well-dated records also have been interpreted as tracking the $\delta^{18}O$ of paleo-precipitation. They exhibit a steady increase in $\delta^{18}O$ values of ~2‰ between the last glacial maximum and the late glacial period, which is particularly prominent in the Fort Stanton speleothem, and a similar increase in $\delta^{18}O$ values between the late glacial and early Holocene, which is captured in all three records. The long-term isotopic trends recorded by these speleothems are similar in temporal range, magnitude, direction, and rate of change to those observed in the San Pedro Valley gastropod $\delta^{18}O$ data. Importantly, there is no discernable difference in the timing of the isotopic changes between the speleothem and gastropod shell records, which would be expected if there was a significant lag between precipitation in the recharge areas and either groundwater discharge in the San Pedro Valley or calcite precipitation at the three speleothem sites. Together, the data suggest that the oxygen isotopic composition of the gastropod shells and speleothems were driven by the same environmental parameters, primarily the $\delta^{18}O$ of precipitation, over millennial timescales during the late Quaternary (Fig. 5).

The results of our study support the use of gastropod shell $\delta^{18}O$ as a paleoclimatic proxy, but with a clear understanding of its limitations and strengths, particularly with regard to the host sediments. The San Pedro Valley gastropod isotopic record exhibits temporal gaps that are consistent with the intermittent nature of groundwater-fed paleowetlands, resulting in chronologic resolution on the order of millennial to sub-millennial timescales. In contrast, the regional speleothem $\delta^{18}O$ data are more continuous and the temporal resolution of all three compared records is

https://doi.org/10.1017/qua.2021.18 Published online by Cambridge University Press

extremely high, exhibiting isotopic variations at centennial and even sub-centennial timescales. Future work should focus on improving the temporal resolution of gastropod shell records by targeting known paleowetland sedimentary sequences that exhibit extremely high rates of sedimentation (e.g., Springer et al., 2015, 2018; Pigati et al., 2019). An additional depositional setting suitable for gastropod shell $\delta^{18}O$ investigations is the thick packages of terrestrial shell-rich glacial age loess, which occur in the midwestern and south-central U.S. (Pigati et al., 2013, 2015; Nash et al., 2018; Grimley et al., 2020). Together, these deposits could provide gastropod shell isotopic records that span large portions of North America.

The worldwide geographic distribution of terrestrial gastropods in the fossil record opens a new avenue of study in which the $\delta^{18}O$ of gastropod shells could be used to examine spatial patterns in the $\delta^{18}O$ of paleo-precipitation at specific snapshots in time over large areas. The data presented here show that isotopic values of gastropod shells in some settings track environmental changes in a manner that is similar to speleothems, but potentially with much greater spatial coverage, although additional studies are needed to realize their full potential as a paleoclimatic proxy.

CONCLUSIONS

Terrestrial gastropod shells are one of the most common fossils in the Quaternary geologic record and are preserved in a wide array of depositional settings. Previous studies of modern taxa have shown that the $\delta^{18}O$ of gastropod shells is driven largely by the $\delta^{18}O$ of precipitation, and therefore the $\delta^{18}O$ of fossil shells could potentially be used to reconstruct the $\delta^{18}O$ of paleo-precipitation, provided the isotopic system of the gastropods and potential hydrologic pathways are well understood. This would allow researchers to obtain paleoclimatic information that is complementary to other geologic proxy records, such as speleothems, and improve our understanding of past climates, particularly in arid environments where long-lived records are relatively rare.

The fossil gastropods studied here, which include Succineidae, *Pupilla hebes*, *Gastrocopta tappaniana*, and *Vallonia gracilicosta*, exhibit differences in $\delta^{18}O$ values of up to ~2‰ between taxa for shells recovered within the same sampling interval, which is nearly identical to inter-taxa differences observed in modern gastropods. Normalized gastropod shell $\delta^{18}O$ values increased by ~4‰ between the last glacial maximum and early Holocene, similar to the magnitude, direction, and rate of change recorded by speleothems in the region during the same period of time. This suggests that both systems are driven by the same environmental parameters, primarily the $\delta^{18}O$ of paleo-precipitation, and that the shells track climatic variability in this region in a manner that is similar to speleothems, albeit currently at coarser temporal resolution.

Constructing $\delta^{18}O$ records based on small gastropod shells allows for large numbers of shells to be analyzed per sampling interval and for systematic differences between taxa to be quantified. Future work is needed to determine if gastropod shell isotope records can be improved by amalgamating shells, rather than analyzing individual shells, much like methods that have been developed for isotopic studies of marine foraminifera (Groeneveld et al., 2019). Additional work is also needed to improve the chronologic control and spatial coverage of $\delta^{18}O$ records derived from gastropod shells by focusing on paleowetland, loess, and other sedimentary sequences that exhibit exceptionally high sedimentation rates at sites throughout the western and central U.S. Such efforts ultimately will enhance our understanding of past climate conditions over large parts of the North American continent during the Quaternary, and will assist in anticipating and preparing for societal impacts of climate change projected for the future.

Supplementary Material. The supplementary material for this article can be found at https://doi.org/10.1017/qua.2021.18

Acknowledgments. We thank associate editor Kathleen Johnson and reviewers David Dettman, Dan Muhs, and an anonymous reviewer for providing constructive comments that greatly improved the quality of the manuscript. We also thank Paco van Sistine (U.S. Geological Survey) for assistance with the site location figure. Any use of trade, product, or firm names is for descriptive purposes only and does not imply endorsement by the U.S. Government. Downloadable files of the data presented in the Supplementary Information can be found at https://doi.org/10.5066/P9EISWFZ.

Financial Support. This project was funded by a National Science Foundation grant (EAR-1529133) and the USGS Climate and Land Use Change Research and Development Program through the Quaternary Hydroclimate Records of Spring Ecosystems project.

REFERENCES

Asmerom, Y., Polyak, V., Burns, S., Rassmussen, J., 2007. Solar forcing of Holocene climate: new insights from a speleothem record, southwestern United States. *Geology* **35**, 1–4.

Asmerom, Y., Polyak, V.J., Burns, S.J., 2010. Variable winter moisture in the southwestern United States linked to rapid glacial climate shifts. *Nature Geoscience* **3**, 114–117.

Asmerom, Y., Polyak, V.J., Lachniet, M., 2017. Extrapolar climate reversal during the last deglaciation. *Nature Scientific Reports* **17**. https://doi.org/10.1038/s41598-41017-07721-41598.

Balakrishnan, M., Yapp, C.J., 2004. Flux balance models for the oxygen and carbon isotope compositions of land snail shells. *Geochimica et Cosmochimica Acta* **68**, 2007–2024.

Balakrishnan, M., Yapp, C.J., Meltzer, D.J., Theler, J.L., 2005a. Paleoenvironment of the Folsom archaeological site, New Mexico, USA, approximately 10,500 ^{14}C yr B.P. as inferred from the stable isotope composition of fossil land snail shells. *Quaternary Research* **63**, 31–44.

Balakrishnan, M., Yapp, C.J., Theler, J.L., Carter, B.J., Wyckoff, D.G., 2005b. Environmental significance of $^{13}C/^{12}C$ and $^{18}O/^{16}O$ ratios of modern land-snail shells from the southern great plains of North America. *Quaternary Research* **63**, 15–30.

Blaauw, M., Christen, J.A., 2011. Flexible paleoclimate age-depth models using an autoregressive gamma process. *Bayesian Analysis* **6**, 457–474.

Cooke, R.U., Reeves, R.W., 1976. *Arroyos and Environmental Change*. Oxford University Press, Oxford, 213 p.

Coplen, T.B., Brand, W.A., Gehre, M., Groning, M., Meijer, H.A.J., Toman, B., Verkouteren, R.M., 2006. New guidelines for ^{13}C measurements. *Analytical Chemistry* **78**, 2439–2441.

Dykoski, C.A., Edwards, R.L., Cheng, H., Yuan, D.X., Cai, Y.J., Zhang, M.L., Lin, Y.S., Qing, J.M., An, Z.S., Revenaugh, J., 2005. A high-resolution, absolute-dated Holocene and deglacial Asian monsoon record from Dongge Cave, China. *Earth and Planetary Science Letters* **233**, 71–86.

Fleitmann, D., Burns, S.J., Mangini, A., Mudelsee, M., Kramers, J., Villa, I., Neff, U., *et al.*, 2007. Holocene ITCZ and Indian monsoon dynamics recorded in stalagmites from Oman and Yemen (Socotra). *Quaternary Science Reviews* **26**, 170–188.

Goldscheider, N., Chen, Z., Auler, A.S., Bakalowicz, M., Broda, S., Drew, D., Hartmann, J., *et al.*, 2020. Global distribution of carbonate rocks and karst water resources. *Hydrogeology Journal* **28**, 1661–1677.

Goodfriend, G.A., Ellis, G.L., 2002. Stable carbon and oxygen isotopic variations in modern *Rabdotus* land snail shells in the southern Great Plains, USA, and their relation to environment. *Geochimica et Cosmochimica Acta* **66**, 1987–2002.

Grimley, D.A., Counts, R.C., Conroy, J.L., Wang, H., Dendy, S.N., Nield, C.B., 2020. Last glacial maximum ecology and climate from terrestrial gastropod assemblages in Peoria loess, western Kentucky. *Journal of Quaternary Science* **35**, 650–663.

Groeneveld, J., Ho, S.L., Mackensen, A., Mohtadi, M., Laepple, T., 2019. Deciphering the variability in Mg/Ca and stable oxygen isotopes of individual foraminifera. *Paleoceanography and Paleoclimatology* **34**, 755–773.

Haynes, C.V., Jr., 1987. Curry Draw, Cochise County, Arizona: a late Quaternary stratigraphic record of Pleistocene extinction and paleo-Indian activities. *Geological Society of America Centennial Field Guide - Cordilleran Section* **1**, 23–28.

Haynes, C.V., Jr., 1968. Preliminary report on the late Quaternary geology of the San Pedro Valley, Arizona. In: Titley, S.R. (Ed.), *Southern Arizona Guidebook III*. Arizona Geological Society, Tucson, AZ, pp. 79–96.

Haynes, C.V., Jr., 2007. Quaternary geology of the Murray Springs Clovis site. In: Haynes, C.V., Jr., Huckell, B.B. (Eds.), *Murray Springs: A Clovis Site with Multiple Activity Areas in the San Pedro Valley, Arizona*. The University of Arizona Press, Tucson, AZ, pp. 16–56.

Hudson, A.M., Hatchett, B.J., Quade, J., Boyle, D.P., Bassett, S.D., Ali, G., DelosSantos, M.G., 2019. North-south dipole in winter hydroclimate in the western United States during the last deglaciation. *Scientific Reports,* **9**, 4826. https://doi.org/10.1038/s41598-019-41197-y.

IPCC, 2014. Climate Change 2014: Synthesis Report. Contribution of Working Groups I, II and III to the Fifth Assessment Report of the Intergovernmental Panel on Climate Change (Core Writing Team, R.K. Pachauri and L.A. Meyer [Eds.]). IPCC, Geneva, Switzerland, 151 pp.

Lachniet, M.S., Denniston, R.F., Asmerom, Y., Polyak, V.J., 2014. Orbital control of western North America atmospheric circulation and climate over two glacial cycles. *Nature Communications* **5**, 3805. http://dx.doi.org/3810.1038/ncomms4805.

Lecolle, P., 1985. The oxygen isotope composition of landsnail shells as a climatic indicator: applications to hydrogeology and paleoclimatology. *Chemical Geology: Isotope Geosciences section* **58**, 157–181.

Lora, J.M., Ibarra, D.E., 2019. The North American hydrologic cycle through the last deglaciation. *Quaternary Science Reviews* **226**, 1–25.

Mead, J.I., 2007. Molluscan faunas of the San Pedro Valley, Arizona. In: Haynes, C.V., Jr., Huckell, B.B. (Eds.), *Murray Springs: A Clovis Site with Multiple Activity Areas in the San Pedro Valley, Arizona*. The University of Arizona Press, Tucson, pp. 62–82.

Metcalfe, S.A., Barron, J.A., Davies, S.J., 2015. The Holocene history of the North American Monsoon: 'known knowns' and 'known unknowns' in understanding its spatial and temporal complexity. *Quaternary Science Reviews* **120**, 1–27.

Nash, T.A., Conroy, J.L., Grimley, D.A., Guenthner, W.R., Curry, B.B., 2018. Episodic deposition of Illinois Valley Peoria silt in association with Lake Michigan Lobe fluctuations during the last glacial maximum. *Quaternary Research* **89**, 739–755.

Paul, D., Mauldin, R., 2013. Implications for Late Holocene climate from stable carbon and oxygen isotopic variability in soil and land snail shells from archaeological site 41KM69 in Texas, USA. *Quaternary International* **308–309**, 242–252.

Pigati, J.S., Bright, J.E., Shanahan, T.M., Mahan, S.A., 2009. Late Pleistocene paleohydrology near the boundary of the Sonoran and Chihuahuan deserts, southeastern Arizona, USA. *Quaternary Science Reviews* **28**, 286–300.

Pigati, J.S., McGeehin, J.P., Muhs, D.R., Bettis, E.A.I., 2013. Radiocarbon dating late Quaternary loess deposits using small terrestrial gastropod shells. *Quaternary Science Reviews* **76**, 114–128.

Pigati, J.S., McGeehin, J.P., Muhs, D.R., Grimley, D.C., Nekola, J.C., 2015. Radiocarbon dating loess deposits in the Mississippi Valley using terrestrial gastropod shells (Polygyridae, Helicinidae, Discidae). *Aeolian Research* **16**, 25–33.

Pigati, J.S., Quade, J., Shanahan, T.M., Haynes, C.V.J., 2004. Radiocarbon dating of minute gastropods and new constraints on the timing of spring-discharge deposits in southern Arizona, USA. *Palaeogeography, Palaeoclimatology, Palaeoecology* **204**, 33–45.

Pigati, J.S., Springer, K.B., Honke, J.S., 2019. Desert wetlands record hydrologic variability within the Younger Dryas chronozone, Mojave Desert, USA. *Quaternary Research* **91**, 51–62.

Polyak, V.J., Asmerom, Y., Burns, S.J., Lachniet, M.S., 2012. Climatic backdrop to the terminal Pleistocene extinction of North American mammals. *Geology* **40**, 1023–1026.

Polyak, V.J., Rasmussen, J.B.T., Asmerom, Y., 2004. Prolonged wet period in the southwestern United States through the Younger Dryas. *Geology* **32**, 5–8.

Quade, J., 2003. Isotopic records from ground-water and cave speleothem calcite in North America. In: Gillespie, A., Porter, S.C., Atwater, B.F. (Eds.), *The Quaternary Period in the United States*. Elsevier Science, New York, pp. 205–220.

Reimer, P.J., Austin, W.E.N., Bard, E., Bayliss, A., Blackwell, P.G., BronkRamsey, C., Butzin, M., *et al.*, 2020. The IntCal20 Northern Hemisphere radiocarbon age calibration curve (0–55 cal kBP). *Radiocarbon* **62**, 725–757.

Reynolds, S.J., 1988. Geologic Map of Arizona. Arizona Geological Survey Map 26, Scale 1:1,000,000.

Spotl, C., Vennemann, T.W., 2003. Continuous-flow isotope ratio mass spectrometric analysis of carbonate minerals. *Rapid Communications in Mass Spectrometry* **17**, 1004–1006.

Springer, K.B., Manker, C.R., Pigati, J.S., 2015. Dynamic response of desert wetlands to abrupt climate change. *Proceedings of the National Academy of Sciences USA* **112**, 14522–14526.

Springer, K.B., Pigati, J.S., Manker, C.R., Mahan, S.A., 2018. The Las Vegas Formation. *U.S. Geological Survey Professional Paper* 1839, 62 p. https://doi.org/10.3133/pp1839.

Stuiver, M., Reimer, P.J., Reimer, R.W., 2020. CALIB 8.2 [WWW program]. http://calib.org. [accessed 2020-8-23]

Vogel, J.S., Southon, J.R., Nelson, D.E., Brown, T.A., 1984. Performance of catalytically condensed carbon for use in accelerator mass spectrometry. *Nuclear Instruments and Methods in Physics Research B* **5**, 289–293.

Wagner, J.D.M., Cole, J.E., Beck, J.W., Patchett, P.J., Henderson, G.M., Barnett, H.R., 2010. Moisture variability in the southwestern United States linked to abrupt glacial climate change. *Nature Geoscience* **3**, 110–113.

Wang, Y.J., Cheng, H., Edwards, R.L., An, Z.S., Wu, J.Y., Shen, C.C., Dorale, J.A., 2001. A high-resolution absolute-dated late Pleistocene monsoon record from Hulu Cave, China. *Science* **294**, 2345–2348.

Waters, M.R., Haynes, C.V., 2001. Late Quaternary arroyo formation and climate change in the American Southwest. *Geology* **29**, 399–402.

Wise, E.K., 2010. Spatiotemporal variability of the precipitation dipole transition zone in the western United States. *Geophysical Research Letters* **37**, L07706. https://doi.org/10.1029/2009GL042193.

Yanes, Y., Al-Qattan, N.M., Rech, J.A., Pigati, J.S., Dodd, J.P., Nekola, J.C., 2019. Overview of the oxygen isotope systematics of land snails from North America. *Quaternary Research* **91**, 329–344.

Yanes, Y., Nekola, J.C., Rech, J.A., Pigati, J.S., 2017. Oxygen stable isotopic disparities among sympatric small land snail species from northwest Minnesota, USA. *Palaeogeography, Palaeoclimatology, Palaeoecology* **485**, 715–722.

Yanes, Y., Riquelme, J.A., Camara, J.A., 2013. Stable isotope composition of middle to late Holocene land snail shells from the Marroques archeological site (Jaen, Southern Spain): paleoenvironmental implications. *Quaternary International* **302**, 77–87.

Yanes, Y., Romanek, C.S., Delgado, A., Brant, H.A., Noakes, J.E., Alonso, M.R., Ibáñez, M., 2009. Oxygen and carbon stable isotopes of modern land snail shells as environmental indicators from a low-latitude oceanic island. *Geochimica et Cosmochimica Acta* **73**, 4077–4099.

Yanes, Y., Yapp, C.J., Ibáñez, M., Alonso, M.R., De la Nuez, J., Quesada, M.L., Castillo, C., Delgado, A., 2011. Pleistocene–Holocene environmental change in the Canary Archipelago as inferred from stable isotopes of land snail shells. *Quaternary Research* **65**, 658–669.

Yapp, C.J., 1979. Oxygen and carbon isotope measurements of land snail shell carbonate. *Geochimica et Cosmochimica Acta* **43**, 629–635.

https://doi.org/10.1017/qua.2021.18 Published online by Cambridge University Press